

The motion of pressure distribution over a free surface near the edge of ice sheet

I V Sturova and L A Tkacheva

Lavrentyev Institute of Hydrodynamics SB RAS, Novosibirsk, Russia

E-mail: sturova@hydro.nsc.ru, tkacheva@hydro.nsc.ru

Abstract. The solution of a steady three-dimensional problem for the wave disturbances induced by a pressure distribution moving with uniform speed along the rectilinear edge of semi-infinite ice sheet is presented. This external load simulates the air-cushion vehicle. The problem is formulated within linear hydroelastic theory. The fluid is assumed to be inviscid and incompressible and its motion is potential. The ice sheet is treated as an elastic thin plate using the Kirchhoff-Love model. The solution of this problem is constructed using the Fourier transform and the Wiener-Hopf technique. The displacements of free surface and ice cover are determined, as well as power characteristics (wave resistance and side force) acting on the vehicle at various speeds of its movement: subcritical and supercritical relative to the minimum phase velocity of flexural-gravity waves in the ice cover. It is found that at speeds close to the critical velocity of flexural-gravity waves, the wave forces undergo sharp changes. It is shown that for some values of load speed, ice thickness and external pressure, the ice fracture near the edge is possible.

1. Introduction

The hydrodynamic aspects of an air cushion vehicle (ACV) can be studied by assuming its action to be equivalent to that of a pressure distribution acting on the free surface of water [1]. The disturbance induced by a pressure distribution moving over infinitely extended free surface has been thoroughly studied (see, e.g. [2]). However, in polar regions of the World Ocean, there are situations when the vehicle moves along the edge of ice sheet. Previously we obtained the solution of a steady three-dimensional problem for flexural-gravity waves generated by a local pressure distribution moving with uniform speed over semi-infinite ice sheet along its rectilinear edge [3] - [6]. Three configurations were considered: (i) the surface of fluid is free outside of ice sheet; (ii) two semi-infinite ice sheets (may be of different thickness) divided by a crack with free edges; (iii) the fluid is bounded by a rigid vertical wall and the edge of an ice sheet can be both free or clamped.

In this paper, the steady problem for the fluid and semi-infinite ice sheet under the action of an external load moving with uniform speed over a free surface along the edge of ice sheet is considered.

2. Mathematical formulation

The water is taken to be of constant density ρ_0 and uniform depth H . The pressure distribution $P(x, y)$ moves with constant speed U over a free surface along the rectilinear edge of the ice sheet. We consider the moving together with the load Cartesian coordinate system (x, y, z) with



x -axis directed perpendicular to the edge of the plate, the y -axis along the edge, and the z -axis vertically upwards. The upper boundary of fluid is covered by an ice sheet in the region $x < 0$ and the surface of fluid is free outside of ice sheet in the region $x > 0$. The fluid motion is irrotational and can be described by a velocity potential $\varphi(x, y, z)$. The ice sheet is assumed isotropic and homogeneous and is treated as an elastic thin plate. It is assumed that the plate is in contact with the water at all points and the plate draft is ignored.

The boundary-value problem for the velocity potential and the free surface elevation or plate deflection $w(x, y)$ can be written as

$$\Delta_3 \varphi = 0 \quad (|x|, |y| < \infty, -H \leq z \leq 0), \quad \Delta_3 \equiv \Delta_2 + \partial^2 / \partial z^2, \quad \Delta_2 \equiv \partial^2 / \partial x^2 + \partial^2 / \partial y^2, \quad (1)$$

$$D \Delta_2^2 w + \rho h U^2 \frac{\partial^2 w}{\partial y^2} + g \rho_0 w - \rho_0 U \frac{\partial \varphi}{\partial y} \Big|_{z=0} = 0 \quad (x < 0), \quad g w - U \frac{\partial \varphi}{\partial y} \Big|_{z=0} = -\frac{P(x, y)}{\rho_0} \quad (x > 0), \quad (2)$$

$$\frac{\partial \varphi}{\partial z} \Big|_{z=0} = -U \frac{\partial w}{\partial y}, \quad \frac{\partial \varphi}{\partial z} \Big|_{z=-H} = 0, \quad (3)$$

$$\left(\frac{\partial^2}{\partial x^2} + \nu \frac{\partial^2}{\partial y^2} \right) w = 0, \quad \frac{\partial}{\partial x} \left[\frac{\partial^2}{\partial x^2} + (2 - \nu) \frac{\partial^2}{\partial y^2} \right] w = 0 \quad (x = 0-, |y| < \infty). \quad (4)$$

Here $D = Eh^3/[12(1 - \nu^2)]$; E , ν , h , ρ are Young's modulus, Poisson's ratio, the thickness and density of ice sheet, respectively; g is the acceleration due to gravity. For wave motion the decaying conditions should be satisfied far from the pressure region.

We restrict our consideration to the pressure distribution in the form

$$P(x, y) = \frac{P_0}{2} \{ \tanh[\varkappa(y + b)] - \tanh[\varkappa(y - b)] \} [\mathcal{H}(x - x_0 + a) - \mathcal{H}(x - x_0 - a)], \quad (5)$$

where P_0 is the nominal pressure, and a and b are respectively the half-beam and half-length of pressure region whose center is located at the point $(x = x_0 > a, y = 0)$, and $\mathcal{H}(\cdot)$ is the Heaviside function. The rate of pressure fall-off at the edges is controlled by the parameter \varkappa . As a special case, $\varkappa \rightarrow \infty$ is equivalent to a uniform pressure acting on a rectangular area: $|x - x_0| \leq a$, $|y| \leq b$. This representation was used in [3] - [6]. However, when the load moves over a free surface, the constant pressure distribution in the rectangular planform leads to unrealistic oscillations in the wave resistance curve at the low Froude numbers [1].

We are interested in bending stresses in the ice cover. In particular, it is of practical interest to know whether the moving load can lead to stresses large enough to break the ice near the edge. The strain tensor $\varepsilon(x, y)$ is given by the matrix

$$\varepsilon(x, y) = -\frac{h}{2} \left\| \begin{array}{cc} \partial^2 w / \partial x^2 & \partial^2 w / \partial x \partial y \\ \partial^2 w / \partial x \partial y & \partial^2 w / \partial y^2 \end{array} \right\|. \quad (6)$$

This tensor describes the strain field in the ice sheet.

The forces F_x (side force) and F_y (wave resistance) acting on ACV and its non-dimensional values A_x , A_y are determined by formulas

$$(R_x, R_y) = - \int_{x_0-a}^{x_0+a} \int_{-\infty}^{\infty} P(x, y) \left(\frac{\partial w}{\partial x}, \frac{\partial w}{\partial y} \right) dy dx, \quad (A_x, A_y) = -\frac{g \rho_0}{2a P_0^2} (R_x, R_y). \quad (7)$$

3. Method of solution

We describe briefly the solution of problem (1)~(4) by the Wiener-Hopf technique. The dimensionless variables and parameters are introduced

$$(x', y', z', a', b', x'_0) = (x, y, z, a, b, x_0) / H, \quad \varkappa' = H \varkappa,$$

$$\beta = D/(\rho_0 g H^4), \quad F = U/\sqrt{gH}, \quad \sigma = \rho h/(\rho_0 H), \quad P'_0 = P_0/(\rho_0 g H).$$

Below, the primes are omitted. We will seek the velocity potential and the displacement in the form $\varphi = UH\phi(x, y, z)$, $w = HW(x, y)$.

We use the Fourier transforms to the variables x and y in the form

$$\Phi_-(\alpha, s, z) = \int_{-\infty}^{\infty} e^{-isy} \int_{-\infty}^0 \phi(x, y, z) e^{i\alpha x} dx dy, \quad \Phi_+(\alpha, s, z) = \int_{-\infty}^{\infty} e^{-isy} \int_0^{\infty} \phi(x, y, z) e^{i\alpha x} dx dy.$$

From the Laplace equation (1) and no-flux bottom condition (3), we have

$$\Phi(\alpha, s, z) = \Phi_- + \Phi_+ = C(\alpha, s)Z(\alpha, s, z), \quad Z = \cosh[(z+1)\sqrt{\alpha^2 + s^2}]/\cosh \sqrt{\alpha^2 + s^2}, \quad (8)$$

where $C(\alpha, s)$ is unknown function. We introduce the functions $F_{\pm}(\alpha, s)$, $G_{\pm}(\alpha, s)$ in the following manner:

$$F_- = \int_{-\infty}^{\infty} e^{-isy} \int_{-\infty}^0 \left(\frac{\partial \phi}{\partial z} + F^2 \frac{\partial^2 \phi}{\partial y^2} \right) \Big|_{z=0} e^{i\alpha x} dx dy, \quad F_+ = \int_{-\infty}^{\infty} e^{-isy} \int_0^{\infty} \left(\frac{\partial \phi}{\partial z} + F^2 \frac{\partial^2 \phi}{\partial y^2} \right) \Big|_{z=0} e^{i\alpha x} dx dy, \quad (9)$$

$$G_- = \int_{-\infty}^{\infty} e^{-isy} \int_{-\infty}^0 \left[\left(\beta \Delta_2^2 + 1 + \sigma F^2 \frac{\partial^2}{\partial y^2} \right) \frac{\partial \phi}{\partial z} + F^2 \frac{\partial^2 \phi}{\partial y^2} \right] \Big|_{z=0} e^{i\alpha x} dx dy, \quad (10)$$

$$G_+ = \int_{-\infty}^{\infty} e^{-isy} \int_0^{\infty} \left[\left(\beta \Delta_2^2 + 1 + \sigma F^2 \frac{\partial^2}{\partial y^2} \right) \frac{\partial \phi}{\partial z} + F^2 \frac{\partial^2 \phi}{\partial y^2} \right] \Big|_{z=0} e^{i\alpha x} dx dy. \quad (11)$$

The functions with indexes $+/-$ are analytical on α in the upper/lower half-plane, respectively. From boundary conditions (2), we have

$$G_-(\alpha, s) = 0, \quad F_+(\alpha, s) = isQ(\alpha, s), \quad (12)$$

where

$$Q(\alpha, s) = \int_{-\infty}^{\infty} \int_{x_0-a}^{x_0+a} P(x, y) e^{i(\alpha x - sy)} dx dy = \frac{2\pi P_0 \sin(\alpha a) \sin(sb)}{\alpha \varkappa \sinh[\pi s/(2\varkappa)]} e^{i\alpha x_0}.$$

Using (8)~(12), we can write

$$F_-(\alpha, s) + isQ(\alpha, s) = C(\alpha, s)K_1(\alpha, s), \quad G_+(\alpha, s) = C(\alpha, s)K_2(\alpha, s), \quad (13)$$

where $K_1(\alpha, s)$ and $K_2(\alpha, s)$ are the dispersion functions for the free surface waves and the flexural-gravity ones in a moving coordinate system, respectively:

$$K_1(\alpha, s) = \sqrt{\alpha^2 + s^2} \tanh \sqrt{\alpha^2 + s^2} - F^2 s^2,$$

$$K_2(\alpha, s) = [\beta(\alpha^2 + s^2)^2 + 1 - \sigma F^2 s^2] \sqrt{\alpha^2 + s^2} \tanh \sqrt{\alpha^2 + s^2} - F^2 s^2.$$

The dispersion relation for free surface waves $\mathcal{K}_1(\gamma) \equiv \gamma \tanh \gamma - F^2 s^2 = 0$ has two real roots $\pm\gamma_0$ and the countable set of imaginary roots $\pm\gamma_m$ ($m = 1, 2, \dots$). The dispersion relation for flexural-gravity waves $\mathcal{K}_2(\mu) \equiv (\beta\mu^4 + 1 - \sigma F^2 s^2)\mu \tanh \mu - F^2 s^2 = 0$ has two real roots $\pm\mu_0$, four complex roots $\pm\mu_{-1}$, $\pm\mu_{-2}$, $\mu_{-2} = -\bar{\mu}_{-1}$ (the bar denotes complex conjugation), and the countable set of imaginary roots $\pm\mu_m$ ($m = 1, 2, \dots$). Then the roots of dispersion functions $K_n(\alpha, s) = 0$ ($n = 1, 2$) are $\chi_m(s) = \sqrt{\gamma_m^2(s) - s^2}$ ($n = 1$) and $\alpha_m(s) = \sqrt{\mu_m^2(s) - s^2}$ ($n = 2$). We take the values of these roots from the upper half-plane.

Excluding the function $C(\alpha, s)$ from equations (13), we obtain

$$F_-(\alpha, s) + isQ(\alpha, s) = G_+(\alpha, s)K(\alpha, s), \quad K(\alpha, s) = K_1(\alpha, s)/K_2(\alpha, s). \quad (14)$$

In accordance with the Wiener-Hopf technique, we factorize the function $K(\alpha, s)$:

$$K(\alpha, s) = K_-(\alpha, s)K_+(\alpha, s), \quad K_{\pm}(\alpha, s) = \frac{\mu_{-1}\mu_{-2}}{(\alpha \pm \alpha_{-1})(\alpha \pm \alpha_{-2})} N_{\pm}(\alpha, s), \quad N_{\pm} = \prod_{j=0}^{\infty} \frac{(\alpha \pm \chi_j)\mu_j}{(\alpha \pm \alpha_j)\gamma_j},$$

where the functions K_{\pm} are analytical in the upper/lower parts of complex plane α , respectively. Dividing (14) by $K_-(\alpha, s)$, we have

$$\frac{F_-(\alpha, s)}{K_-(\alpha, s)} + \frac{\Omega(s)\psi(\alpha)}{K_-(\alpha, s)} = G_+(\alpha, s)K_+(\alpha, s),$$

where

$$\Omega(s) = \frac{\pi s P_0 \sin(sb)}{\varkappa \sinh[\pi s/(2\varkappa)]}, \quad \psi(\alpha) = \frac{e^{i\alpha(x_0+a)} - e^{i\alpha(x_0-a)}}{\alpha}.$$

Then we use the representation

$$\frac{\psi(\alpha)}{N_-(\alpha, s)} = L_+(\alpha, s) + L_-(\alpha, s), \quad L_{\pm}(\alpha, s) = \pm \frac{1}{2\pi i} \int_{-\infty \mp i\lambda}^{\infty \mp i\lambda} \frac{\psi(\zeta)d\zeta}{(\zeta - \alpha)N_-(\zeta, s)},$$

and as a result we obtain the equation

$$\begin{aligned} \frac{F_-(\alpha, s)}{K_-(\alpha, s)} + \Omega(s) \frac{(\alpha - \alpha_{-1})(\alpha - \alpha_{-2})}{\mu_{-1}\mu_{-2}} L_-(\alpha, s) = \\ G_+(\alpha, s)K_+(\alpha, s) - \Omega(s) \frac{(\alpha - \alpha_{-1})(\alpha - \alpha_{-2})}{\mu_{-1}\mu_{-2}} L_+(\alpha, s). \end{aligned}$$

The functions on the left-hand and right-hand sides of this equation are analytical in the lower and upper parts of complex plane α , respectively. Then we have analytical function over the entire complex plane α . By Liouville's theorem, this function is a polynomial. The degree of the polynomial is determined by the behavior of this function as $|\alpha| \rightarrow \infty$ and is equal to one. Consequently, we can write

$$G_+(\alpha, s)K_+(\alpha, s) - \Omega(s) \frac{(\alpha - \alpha_{-1})(\alpha - \alpha_{-2})}{\mu_{-1}\mu_{-2}} L_+(\alpha, s) = \Omega(s)[a_0(s) + a_1(s)\alpha],$$

where $a_0(s)$ and $a_1(s)$ are unknown functions which are defined from edge conditions (4).

The deflection of the plate and the free surface elevation are determined by performing the inverse Fourier transform:

at $x < 0$

$$\begin{aligned} W(x, y) = -\frac{1}{2} \int_{-\infty}^{\infty} e^{isy} \Omega_1(s) \sum_{j=-2}^{\infty} \frac{\mu_j \text{th} \mu_j e^{-i\alpha_j x}}{K_+(\alpha_j, s) K_2'(\alpha_j, s)} \left[a_0(s) + a_1(s) \alpha_j + \right. \\ \left. \frac{(\alpha_j - \alpha_{-1})(\alpha_j - \alpha_{-2})}{\mu_{-1}\mu_{-2}} \sum_{m=0}^{\infty} \frac{\psi(\chi_m)}{(\chi_m - \alpha_j) N_-'(\chi_m, s)} \right] ds, \quad \Omega_1(s) = \frac{\Omega(s)}{\pi s}, \end{aligned}$$

at $x > 0$

$$W(x, y) = -\frac{F^2}{2} \int_{-\infty}^{\infty} e^{isy} s^2 \Omega_1(s) \sum_{j=0}^{\infty} \frac{e^{i\chi_j x} K_+(\chi_j, s)}{K_1'(\chi_j, s)} \left[a_0(s) - a_1(s) \chi_j + \frac{(\chi_j + \alpha_{-1})(\chi_j + \alpha_{-2})}{\mu_{-1}\mu_{-2}} \sum_{m=0}^{\infty} \frac{\psi(\chi_m)}{(\chi_m + \chi_j)N_-'(\chi_m, s)} \right] ds - \frac{F^2}{2} \int_{-\infty}^{\infty} e^{isy} s^2 \Omega_1(s) \Lambda(x, s) ds,$$

where

$$\Lambda(x, s) = \sum_{j=0}^{\infty} \frac{1}{\chi_j K_1'(\chi_j, s)} \begin{cases} \exp[i\chi_j(x_0 - x + a)] - \exp[i\chi_j(x_0 - x - a)] & (0 < x < x_0 - a), \\ \exp[i\chi_j(x_0 - x + a)] + \exp[i\chi_j(x - x_0 + a)] - 2 & (|x - x_0| < a), \\ \exp[i\chi_j(x - x_0 + a)] - \exp[i\chi_j(x - x_0 - a)] & (x > x_0 + a), \end{cases}$$

where the prime denotes the partial derivative of a function with respect to its first variable.

Using free-edge conditions (4), we obtain the system of two linear algebraic equations to define the coefficients $a_0(s)$ and $a_1(s)$. All integrals on α are evaluated by the residue method. The analysis of dispersion relation for free surface waves shows that at any speed of the load there is a value s_0 , that $\gamma_0(s) < |s|$ at $|s| < s_0$ and $\gamma_0(s) > |s|$ at $|s| > s_0$, in this case χ_0 is real. Gravity waves spread at $|s| > s_0$. At $U \geq U_c \equiv \sqrt{gH}$, we have $s_0 = 0$. The velocity U_c is called the limit of long waves.

For the infinitely extended elastic plate, there is a minimum phase velocity of flexural-gravity waves c_m and always $c_m < U_c$ (see, e.g. [7]). If $U < c_m$, then $\mu_0(s) < |s|$ for any values of the parameter s , and the real roots of dispersion relation $K_2(\alpha, s) = 0$ are absent. If $c_m < U < U_c$, then there are two values s_1 and s_2 such that $\mu_0(s) > |s|$ at $s_1 < s < s_2$, in this case α_0 is real. Flexural-gravity waves extend back and forward in the plate for $s_1 < |s| < s_2$. With increasing speed of the load, the value s_1 decreases, and the value s_2 increases. At a speed greater than the long-wave limit U_c , we have $s_1 = 0$.

4. Numerical results

The following input data are used for water, ice sheet and external load: $E = 5GPa$, $\nu = 1/3$, $\rho_0 = 10^3 \text{ kg/m}^3$, $\rho = 900 \text{ kg/m}^3$, $P_0 = 10^3 Pa$, $a = 10 \text{ m}$, $b = 20 \text{ m}$, $x_0 = 50 \text{ m}$, $\varkappa = 5/b$, $H = 100 \text{ m}$. The speed of load U and the thickness of ice sheet h vary in the calculations. The minimum phase velocity of the flexural-gravity waves in infinitely extended ice cover increases with increasing ice thickness and for $h = 0.5, 1, 2 \text{ m}$ is equal to $c_m \approx 12.06, 15.59, 20.09 \text{ m/s}$, respectively. The long-wave limit U_c is approximately equal to 31.32 m/s .

Figure 1 shows the three-dimensional plots for the vertical displacements of free surface at $x > 0$ and ice sheet at $x < 0$ for the motion of load at speed $U = 15 \text{ m/s}$ and different ice thicknesses: $h = 0.5 \text{ m}$ (Fig. 1(a)) and $h = 1 \text{ m}$ (Fig. 1(b)). The load moves from left to right. The load speed is supercritical for an ice cover 0.5 m thick and wave motions are excited in the ice cover, extending to a sufficiently large distance from the edge of ice cover. In the case of thicker ice, $h = 1 \text{ m}$, the load speed is subcritical and in the ice cover only weak wave motions appear decaying rapidly away from the edge. The waves in fluid near the ice cover are weaker for the thinner ice because waves in the plate are greater and absorb stronger energy.

The free surface elevation and ice deflection at $x = 0$ are shown in Fig. 2(a) for $U = 15 \text{ m/s}$ and $h = 1 \text{ m}$. We can see that the lengths of surface waves and flexural-gravity ones differ substantially near the edge of ice cover. On the free surface, the superposition of waves reflected from the edge of ice cover and generated by the pressure region occurs.

The strains along the edge of ice sheet at $x = 0$ for $h = 1 \text{ m}$ and two different speeds of load $U = 10, 15 \text{ m/s}$ are shown in Fig. 2 (b). To find the maximum strain in the ice sheet, we need to find the largest eigenvalue of the strain tensor (6) at each location. The strains

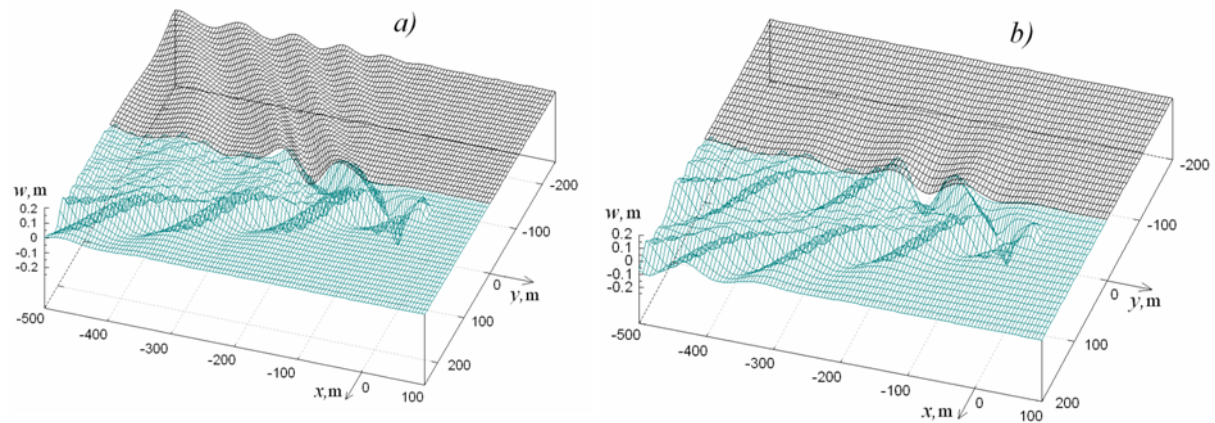


Figure 1. Wave patterns of ice cover ($x < 0$) (gray) and free surface ($x > 0$) (blue) for the load moving with speed $U = 15$ m/s and ice thickness $h = 0.5$ m (a) and $h = 1$ m (b).

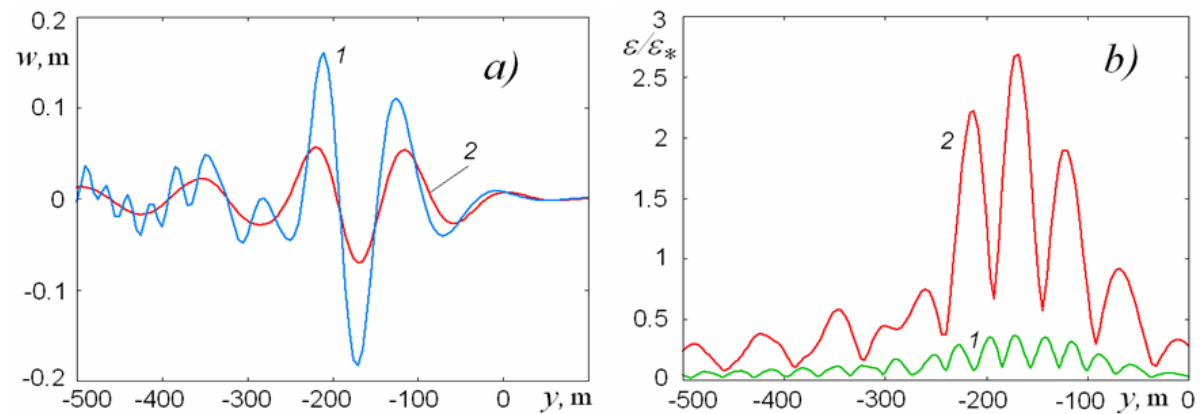


Figure 2. (a) Free surface elevation (1) and the deflection of ice sheet (2) along the ice edge at $x = 0$, $U = 15$ m/s, $h = 1$ m. (b) Strains $\varepsilon/\varepsilon_*$ along the ice edge at $x = 0$ for $h = 1$ m: $U = 10$ m/s (1) and $U = 15$ m/s (2).

are proportional to the magnitude P_0 of external load within the linear theory. The strains are scaled with $\varepsilon_* = 8 \cdot 10^{-5}$, where ε_* is the yield strain at which a material begins to deform plastically. According to [8], any strains greater than the yield strain ε_* are assumed to lead to ice fracture. We can see that at $U = 10$ m/s, $h = 1$ m and at given value of the external load P_0 , ice does not break whereas at speed $U = 15$ m/s and the same values h and P_0 the arising strains exceed the value ε_* and the destruction of ice can be possible.

Non-dimensional values of wave forces A_x and A_y in (7) acting on moving vehicle are presented in Fig. 3 as functions of the load speed. It is known (see e.g. [1]) that when the pressure region (5) moves along an unbounded free surface, side force R_x in (7) is identically zero and wave resistance R_y is

$$R_y = \frac{2\pi P_0^2 F}{\rho_0 g H \chi^2} \int_{K_0}^{\infty} \frac{\sin^2\left(\frac{b}{FH} \sqrt{k \tanh k}\right) \sqrt{k \tanh k}}{(F^2 k - \tanh k)^{3/2} \sinh^2\left(\frac{\pi}{2FH\chi} \sqrt{k \tanh k}\right)} \sin^2\left(\frac{a}{FH} \sqrt{k(F^2 k - \tanh k)}\right) dk, \quad (15)$$

where K_0 is the real positive root of equation $K_0 F^2 = \tanh K_0$ if $F < 1$ while $K_0 = 0$ if $F > 1$.

When the pressure region moves along the edge of ice cover, the side force arises at speeds of load movement close to critical velocity c_m for given ice thickness. As the speed of load increases,

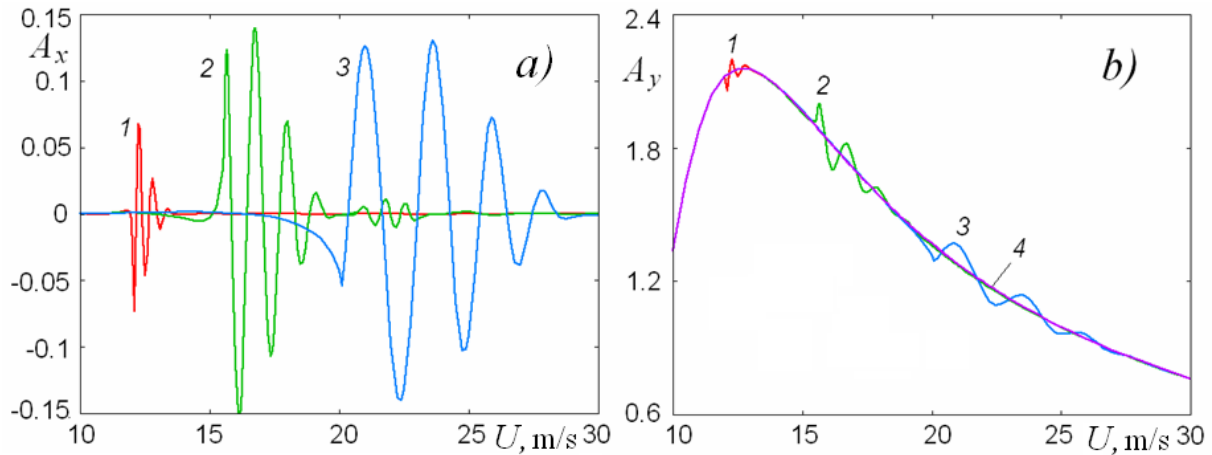


Figure 3. The non-dimensional values of side force A_x (a) and wave resistance A_y (b) for semi-infinite ice sheet with different thickness: curves (1-3) correspond to $h = 0.5, 1, 2$ m. Curve 4 shows the wave resistance for infinite free surface (15).

the side force decreases and tends to zero in an oscillatory manner. The greatest difference of the wave resistance from its value for infinite free surface is observed also at near-critical values of load speed. For subcritical speeds, the disturbances spread only behind the load and do not influence on the vehicle. If $U > c_m$, flexural-gravity waves extend forward in the plate and disturb the fluid near the vehicle. With increasing of speed, the waves in the plate spreading forward become shorter and of smaller amplitude and the influence of ice cover on wave forces decreases.

5. Conclusion

The three-dimensional linear hydroelastic problem on the waves induced by a uniformly moving load over a free surface along the rectilinear edge of a semi-infinite ice sheet is solved. This problem arises, for example, for the air cushion vehicle. The solution is obtained by using the Fourier transform and the Wiener-Hopf technique. The vertical displacements of ice cover and fluid, and wave forces acting on a moving vehicle are defined for different values of the load speed. The speed of the load is shown to affect strongly the response of ice cover. The response is maximum for the load speeds close to the critical speed of hydroelastic waves in infinitely extended ice cover. Wave forces sharply oscillate when the speed of motion is near-critical. It is shown that under certain conditions, the ice at the edge of ice sheet can fracture.

References

- [1] Doctors L J and Sharma S D 1972 *J. Ship Research* **16** 248
- [2] Wehausen J V and Laitone E V 1960 *Surface Waves* (Handbuch der Physik) **9** 446
- [3] Sturova I V and Tkacheva L A 2017 *J. Phys.: Conf. Series* **894**
- [4] Sturova I V 2018 *Fluid Dyn.* **53** 49
- [5] Tkacheva L A 2018 *J. Appl. Mech. Tech. Phys* **59** 258
- [6] Tkacheva L A 2018 *Fluid Dyn.* (accepted)
- [7] Kheysin D Ye 1967 *Dynamics of Floating Ice Covers* (Leningrad, Gidrometeoizdat) (in Russian)
- [8] Brocklehurst P, Korobkin A A and Parau E I 2010 *J. Eng. Math* **68** 215